Materials Research Express

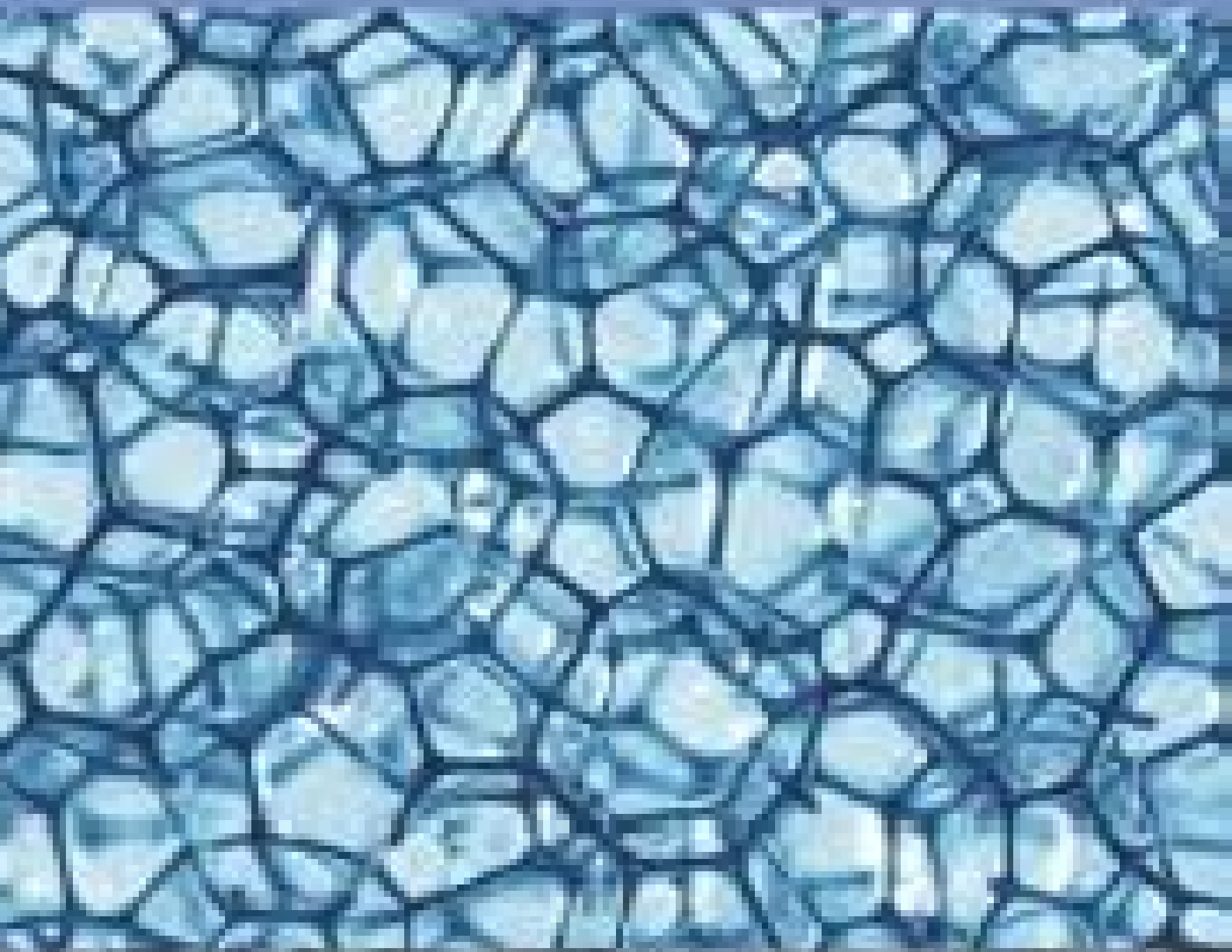

IOP Publishing

Focus on the Indonesian Materials Research Society

Satria Z. Bisri, *RIKEN Center for Emergent Matter Science, Japan*
K Khairurrijal, *Institut Teknologi Bandung, Indonesia*
Rino R. Mukti, *Institut Teknologi Bandung, Indonesia*
Hutomo Suryo Wasisto, *Technische Universitaet Braunschweig, Germany*
Ariando, *National University of Singapore, Singapore*

MRS Indonesia logo supplied by, and re-used with permission from, the MRS-Id Meetings Organising Committee.

We are proud to announce a collaboration between *Materials Research Express* and the Indonesian Materials Research Society (MRS-Id) to recognise the rapid growth of materials science in Indonesia, and its importance to the international materials landscape. *Materials Research Express* presents this exclusive collection of invited papers to showcase the cutting-edge, novel research being undertaken by materials scientists and engineers in this active and diverse region.

Focus Papers

Effects of strain on electronic and optical properties of $LiNbO_3$: a first principles study

R Husin *et al* 2019 *Mater. Res. Express* **6** 114002

+ Open abstract View article PDF

Argon-atmospheric sintering process of stainless steel 17-4 precipitation hardening from metal injection molding product

S Supriadi *et al* 2019 *Mater. Res. Express* **6** 094010

+ Open abstract View article PDF

Preparation and antibacterial properties of cetylpyridinium bromide-modified silver-loaded kaolinite

Nik Ahmad Nizam Nik Malek and Nur Isti'anah Ramli 2019 *Mater. Res. Express* **6** 094006

+ Open abstract View article PDF

The role of tetraalkylammonium for controlling dealumination of zeolite Y in acid media

Ainul Maghfirah *et al* 2019 *Mater. Res. Express* **6** 094002

+ Open abstract View article PDF

OPEN ACCESS

Adhesiveness of TiO_2 PVD coating on electropolished stainless steel 17–4 PH orthodontic bracket

S Supriadi *et al* 2019 *Mater. Res. Express* **6** 094003

+ Open abstract View article PDF

Effect of Au nanoparticles and Au mesostars on the photocatalytic activity of ZnO nanorods

Anita EkaPutri *et al* 2019 *Mater. Res. Express* **6** 084008

+ Open abstract View article PDF

Understanding the role of organic cations on the electronic structure of lead iodide perovskite from their UV photoemission spectra and their electronic structures calculated by DFT method

Yolla Sukma Handayani *et al* 2019 *Mater. Res. Express* **6** 084009

+ Open abstract View article PDF

Gold mesocauliflowers as catalyst for the hydrogenation of acetone to isopropanol

Vivi Fauzia *et al* 2019 *Mater. Res. Express* **6** 084002

+ Open abstract View article PDF

Spillover effect on Pd-embedded metal-organic frameworks based on zirconium(IV) and benzene 1,3,5-tricarboxylate as hydrogen storage materials

Witri Wahyu Lestari *et al* 2019 *Mater. Res. Express* **6** 084001

+ Open abstract View article PDF

Comparison study on molybdena-titania supported on TUD-1 and TUD-C synthesized via sol-gel templating method: Properties and catalytic performance in olefins epoxidation

Yee Khai Ooi *et al* 2019 *Mater. Res. Express* **6** 074001

+ Open abstract View article PDF

Effect of strontium on the microstructure and mechanical properties of aluminium ADC12/Nano-SiC composite with Al-5TiB grain refiner by stir casting method

Anne Zulfia and Lely Tri Putriana 2019 *Mater. Res. Express* **6** 074002

+ Open abstract View article PDF

Response surface methodology to optimize the performance of reduced graphene oxide-mesoporous carbon nitride photocatalysts

Leny Yuliati *et al* 2019 *Mater. Res. Express* **6** 074004

+ Open abstract View article PDF

Luminescent group 11 3, 5-dimethyl pyrazolate complexes/titanium oxide composites for photocatalytic removal and degradation of 2, 4-dichlorophenoxyacetic acid

Hendrik O Lintang *et al* 2019 *Mater. Res. Express* **6** 064001

+ Open abstract View article PDF

Polyvinylpyrrolidone/cellulose acetate nanofibers synthesized using electrospinning method and their characteristics

Jaidan Jauhari *et al* 2019 *Mater. Res. Express* **6** 064002

+ Open abstract View article PDF

Preparation of (002)-oriented ZnO for CO gas sensor

F. Fitriana *et al* 2019 *Mater. Res. Express* **6** 064003

+ Open abstract View article PDF

The effect of annealing and stretching parameters on the structure and performance of polypropylene hollow fiber membrane

A A I A S Komaladewi *et al* 2019 *Mater. Res. Express* **6** 054001

+ Open abstract View article PDF

Materials Research Express

PAPER

Luminescent group 11 3, 5-dimethyl pyrazolate complexes/titanium oxide composites for photocatalytic removal and degradation of 2, 4-dichlorophenoxyacetic acid

RECEIVED
12 December 2018

REVISED
22 January 2019

ACCEPTED FOR PUBLICATION
8 February 2019

PUBLISHED
6 March 2019

Hendrik O Lintang[1,2,3], **Nurul Husna Sabran**[4], **Siew Ling Lee**[3,4] and **Leny Yuliati**[1,2,3]

[1] Ma Chung Research Center for Photosynthetic Pigments, Universitas Ma Chung, Villa Puncak Tidar N-01, Malang 65151, East Java, Indonesia
[2] Department of Chemistry, Faculty of Science and Technology, Universitas Ma Chung, Villa Puncak Tidar N-01, Malang 65151, East Java, Indonesia
[3] Centre for Sustainable Nanomaterials, Ibnu Sina Institute for Scientific and Industrial Research, Universiti Teknologi Malaysia, 81310 UTM Johor Bahru, Johor, Malaysia
[4] Department of Chemistry, Faculty of Science, Universiti Teknologi Malaysia, 81310 UTM Johor Bahru, Johor, Malaysia

E-mail: hendrik.lintang@machung.ac.id

Keywords: degradation, 2, 4-dichlorophenoxyacetic acid, group 11 metal complexes, luminescence, titanium oxide composite

Abstract

We report the successful preparation of new luminescent group 11 pyrazolate complex/titanium oxide composites for the significant improvement of photocatalytic activity in the removal and degradation of 2, 4-dichlorophenoxyacetic acid (2, 4-D). Photocatalyst composites were successfully prepared using an impregnation method of all complexes (M(I or II)) in weight ratios of 0.1–1.0 wt% to TiO_2. In contrast to anatase TiO_2 with 49% for removal and 10% for degradation, the composites Au(I)/TiO_2 and Ag(I)/TiO_2 with 0.4 wt% gave the highest removal and degradation in 85% and 36% in 1 h. Interestingly, the composite Cu(I)/TiO_2 with 0.4 wt% gave even better removal in 99% and almost the same percentage of degradation. By using the same ligand for the complexation, the photocatalyst composite Cu(II)/TiO_2 with the same composition was found to show enhancement in the degradation from 36% to 48% with similar percentage of the removal. These results showed that group 11 pyrazolate complexes in TiO_2 composites could able to significantly improve the photocatalytic activity due to the reduction of electron-hole recombination of TiO_2. Moreover, Cu(I) pyrazolate with longer metal-metal distance (emission peak at 590 nm) for electron transfer from the conduction band is responsible for such performance in the removal. Indeed, dinuclear Cu(II) pyrazolate complex with less rigid structure has more longer metal-metal distance (566 nm) to give such better performance in the degradation. This work demonstrated that modification of TiO_2 with group 11 pyrazolate complexes at the molecular level as photocatalyst composites is a new approach to enhance photocatalytic activity.

1. Introduction

Since last few decades, titanium oxide (TiO_2) has been widely used as a photocatalyst for the degradation of organic pollutants due to its high stability and non-toxicity as well as bandgap energy [1–3]. However, the activity cannot be significantly improved so far [3]. Thus, a lot of studies have been developed to modify TiO_2 as photocatalyst composites with high photocatalytic activity. These composites are generally prepared with the expectation that electron-hole recombination process can be reduced while energy band gap can be improved [4–7].

Recently, transition metal oxides have received special attention among the researchers in the development of photocatalyst composites with good catalytic activity [8–14]. These reports have not yet significantly improved the photocatalytic activity. We have recently reported a new approach to enhance the performance of

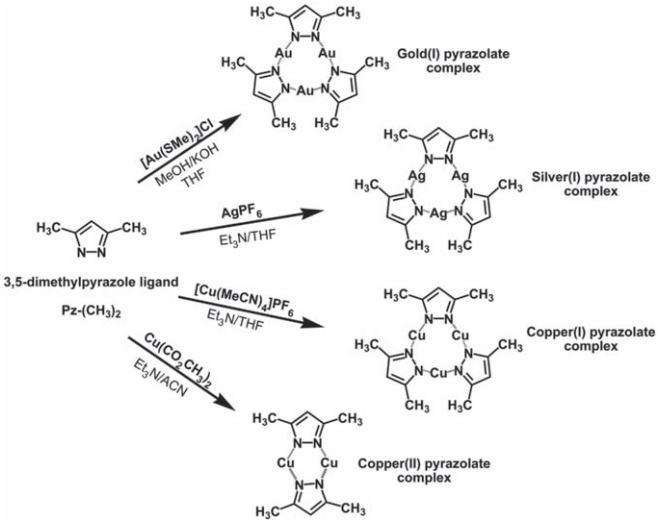

Figure 1. Synthetic scheme of metal(I or II) pyrazolate complexes.

TiO_2 by using columnar assembly of luminescent copper(I) pyrazolate complexes [15]. In this finding, Degussa P25 TiO_2 composite with less rigid structure of 3, 5-dimethyl pyrazole ligand showed more active as a photocatalyst with improvement of photocatalytic activity (in 60%) for the degradation of 2, 4-dichlorophenoxyacetic acid (2, 4-D) as model pollutants compared to the bulk one of 4-(3, 5-dimethoxybenzyl)-3, 5-dimethyl pyrazole ligands (49%) [15]. Since other group 11 pyrazolate complexes also showed similar luminescent properties with copper complexes based on oxidation number of metal ions and distance of the weak metal-metal interactions [16–20], new luminescent composites with a cheaper precursor and stable structure will be highly required as a new photocatalyst. Therefore, we report the first example of photocatalyst composites of modified anatase TiO_2 from group 11 metal complexes for the photocatalytic removal and degradation of 2, 4-D. In this study, we particularly highlight the contribution of different metal complexes from group 11 with different molecular structures as well as the importance of oxidation state of the metal complexes towards the performance of TiO_2 photocatalyst composites.

2. Materials and methods

2.1. Materials

Commercial Hombikat UV100 TiO_2 (anatase TiO_2) from Sachtleben Chemie was used without further treatment. 3, 5-dimethylpyrazole ligand (Sigma-Aldrich, $C_5H_8N_2$, 99%) and metal salts of tetrakis(acetonitrile) copper(I) hexafluorophosphate (Sigma-Aldrich, $C_8H_{12}CuF_6N_4P$, 97%), copper(II) acetate (Sigma-Aldrich, $C_4H_6CuO_4$, 98%), chloro(dimethylsulfide) gold(I) (Sigma-Aldrich, C_2H_6SAuCl), and silver hexafluorophosphate (Sigma-Aldrich, $AgPF_6$, 98%) were used as precursors to synthesize group 11 metal (M(I or II); M = Au, Ag and Cu) pyrazolate complexes. Dry acetonitrile, methanol and tetrahydrofuran for the synthesis were directly used. Triethylamine was firstly distilled under vacuum and an inert condition where it was collected in the round bottom flask containing potassium hydroxide. 2, 4-D ($C_8H_6Cl_2O_3$, 98%) from Sigma-Aldrich was used as a model of organic pollutant.

2.2. Synthesis of luminescent group 11 metal pyrazolate complexes

M(I) pyrazolate complexes were synthesized by mixing 3, 5-dimethylpyrazole ligand (Pz-$(CH_3)_2$) with metal salts in dry solvents using a Schlenk technique under an inert condition as shown in figure 1 [15–19]. Moreover, copper(II) pyrazolate complex was synthesized using copper (II) acetate as the source of metal ion with a certain modification in the synthesis procedure [20]. Typically, the mixture solution of Pz-$(CH_3)_2$ and metal salts was stirred for 5 mins and followed by addition of potassium hydroxide in methanol or fresh distilled triethylamine as a base. After overnight reaction, the solvent was completely removed from the residue using a vacuum pump in high pressure. The remaining residue was further purified using *in situ* recrystallization to obtain targeted complex by adding dichloromethane in small amount for dissolving the residue (desired product). The mixture solution was transferred into dry cold methanol (around 10 times of dichloromethane) to obtain a precipitate. The remaining solvent was removed by *in situ* filtration and further dried using vacuum pump pressure to give white powder of Au(I) pyrazolate complex in 82%, light grey powder of Ag(I) pyrazolate complex in 81%, light

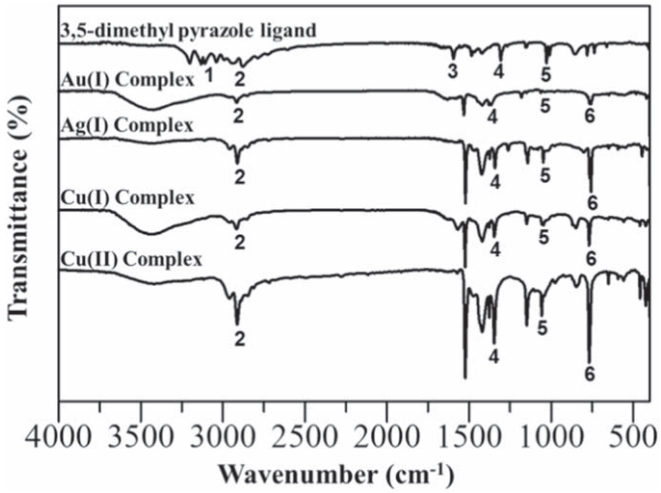

Figure 2. FT-IR spectra of 3, 5-dimethyl pyrazole ligand, Au(I), Ag(I), Cu(I) and Cu(II) pyrazolate complexes.

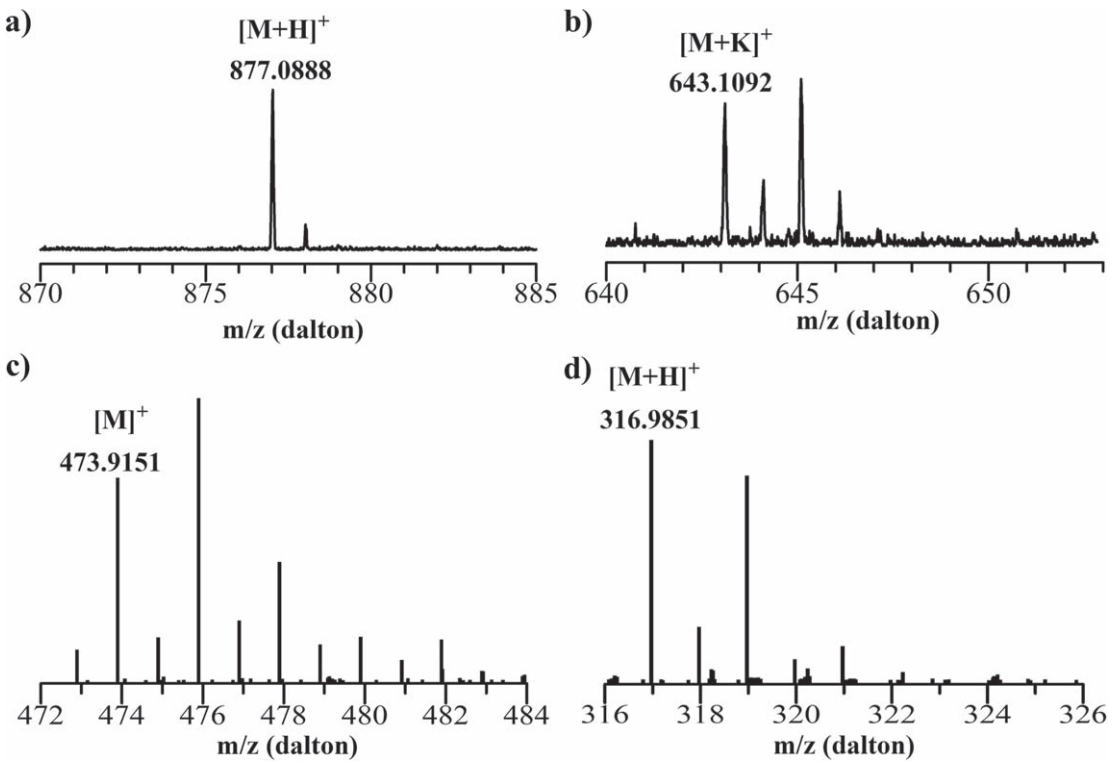

Figure 3. Mass spectra of (a) Au(I), (b) Ag(I), (c) Cu(I) and (d) Cu(II) pyrazolate complexes.

greenish powder of Cu(I) pyrazolate complex in 80%, and light blue-greenish powder of Cu(II) pyrazolate complex in 78%.

2.3. Synthesis of luminescent group 11 metal pyrazolate complexes/titanium oxide composites

Group 11 metal pyrazolate complexes/titanium oxide composites (x-M(I or II)/TiO_2) were prepared as photocatalyst composites using an impregnation method where x represents the weight ratio of M(I or II) pyrazolate complexes to anatase TiO_2 from 0.1 to 1.0 wt%. In this step, TiO_2 (1.0 g) was dispersed to the dichloromethane solution (25 ml) of M(I or II) pyrazolate complexes. The mixture was then sonicated for 20 mins for better dispersion of the complex and TiO_2 [15, 17, 19]. Then, the mixture was stirred until dried at room temperature and calcined at 373 K for 4 hs with heating rate of 10 K min^{-1}.

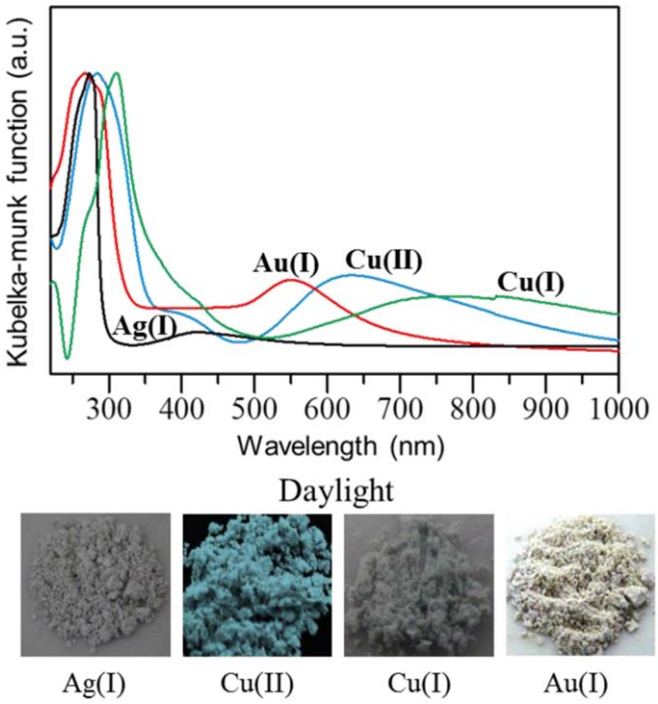

Figure 4. DRUV spectra of Au(I), Ag(I), Cu(I) and Cu(II) pyrazolate complexes and their photographs at daylight.

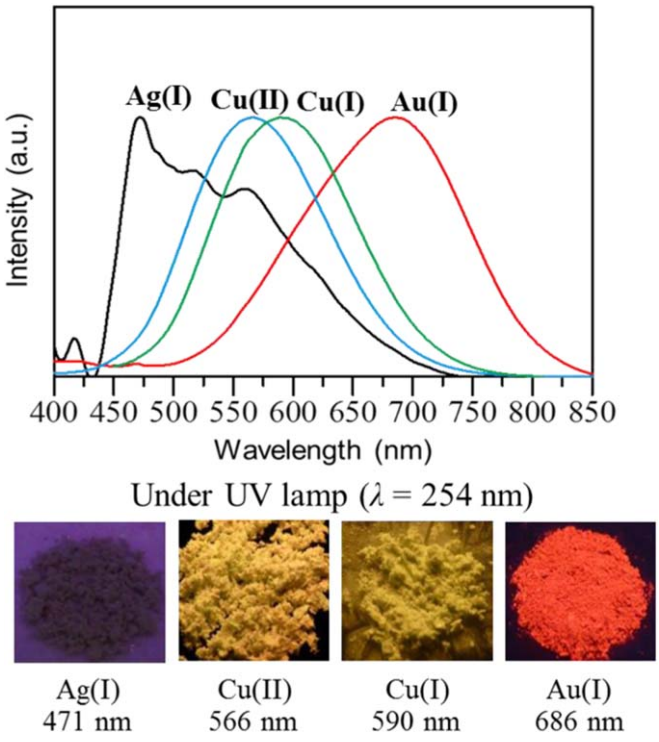

Figure 5. Emission spectra and images of Au(I), Ag(I), Cu(I) and Cu(II) pyrazolate complexes at dark room under exposure UV hand lamp at 254 nm.

2.4. Characterization of luminescent group 11 metal pyrazolate complexes and titanium oxide composites

The M(I or II) pyrazolate complexes and *x*-M(I or II)/TiO_2 composites were characterized with various type of instruments. Fourier transform infrared spectroscopy (FT-IR) on a model of Nicolet iS50 Thermo Scientific was used to analyze M(I or II) pyrazolate complexes using potassium bromide pellet technique. Mass spectra of pyrazolate complexes were analyzed for exact mass analysis using an Agilent 6560 high performance liquid

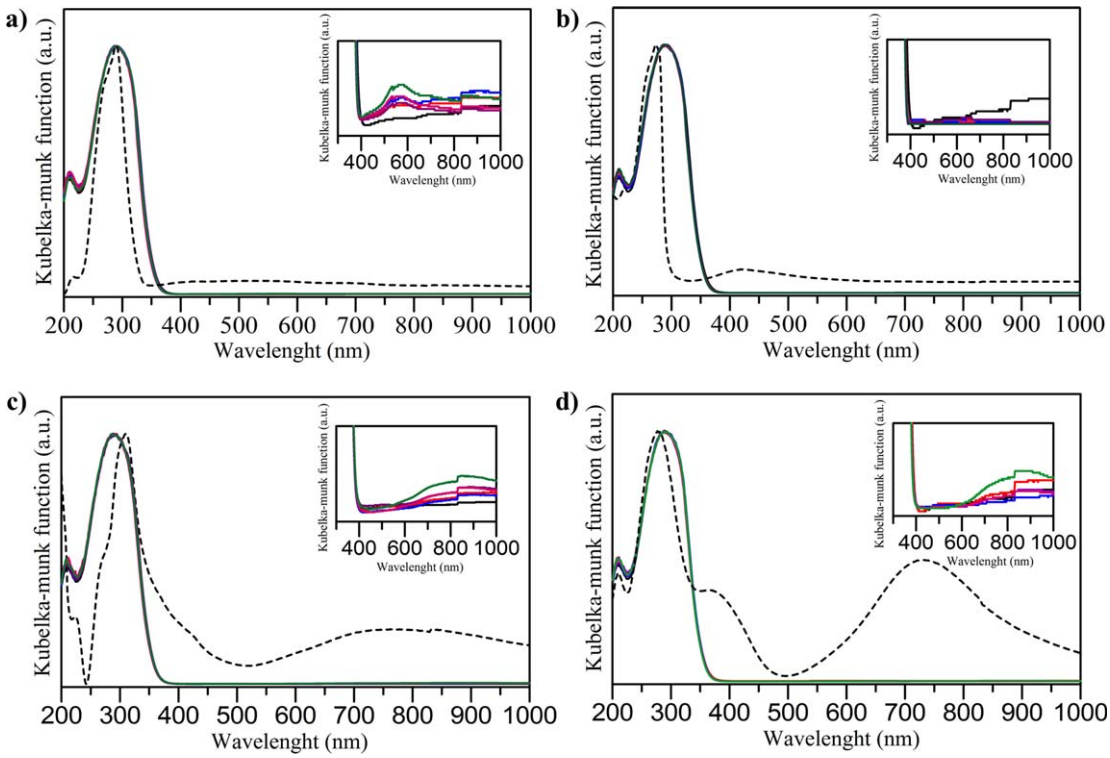

Figure 6. Absorption spectra of (a) Au(I), (b) Ag(I), (c) Cu(I) and (d) Cu(II) pyrazolate complexes (black dashed line), anatase TiO_2 (black line) and photocatalyst composites (0.1, 0.2, 0.4, 0.8, 1.0-M(I or II)/TiO_2; red, blue, purple, orange and green lines).

chromatography tandem mass spectrometry with quadrapole time-of-flight (HP LCMS-MS Q-TOF). The diffraction pattern and crystallite structure of the composites were characterized using Bruker D8 X-ray Diffractometer with a scan speed of 0.05 $°s^{-1}$. The absorption properties were recorded on a DR-UV spectrophotometer (Shimadzu UV-2600) where barium sulphate was used as the reference. JASCO FP-8500 spectroflourophotometer was used to analyze emission properties of the composites.

The morphology of the composites was studied using field emission scanning electron microscopy (FESEM, JEOL on a model of JSM-6701F) operated at 5 kV on samples coated with Pt. FESEM was attached with a spectrometer for element measurement (energy dispersive x-ray, EDX). Transmission electron microscopy (TEM, JEOL) was also performed on a model of JEM-2100 at an accelerating voltage of 200 kV. In the dark room, digital camera on a model of DMC–FZ38 (Panasonic) were used to take photographs under exposure to a hand-held UV lamp ($\lambda_{ex} = 254$ nm).

Photocurrent measurement was performed using an Interface 1000 potentiostat/galvanostat (Gamry Instruments Inc.) with chronoamperometry method. Screen-printed electrode (SPE) as a working electrode was prepared in saturated Na_2SO_4 (0.1 M, 6 ml) solution as an electrolyte. A Xe–Hg UV lamp (200 W, 8 $mWcm^{-2}$) was used as the light source to irradiate the SPE substrate coated with sample. The SPE substrate containing of coated sample was prepared by depositing the mixture of homogeneous colloidal suspension (20 μL) of Nafion (10 μL) with photocatalyst composite (10 mg) in 1 ml of deionized water [12]. The droplet sample was naturally dried under ambient temperature until it was dried-off enough for that photocurrent measurement. The SPE substrate coated with the sample was then applied in the electrolyte system with light-on and off event in every 30 s.

2.5. Characterization of luminescent group 11 metal pyrazolate complexes and titanium oxide composites

The prepared photocatalyst luminescent composites of group 11 metal pyrazolate complexes/titanium oxide (x-M(I or II)/TiO_2) were tested for the removal and degradation of 2, 4-D under a UV light irradiation [6, 13]. x-M(I or II)/TiO_2 in 50 mg was added to the 50 ml solution of 2, 4-D with concentration of 0.5 mM. The mixture was stirred under dark condition for 1 h to reach the adsorption-desorption equilibrium. After that, the mixture was further stirred under UV irradiation (200 W Xe-Hg lamp equipped with IR cut off filter) with light intensity of 8 $mWcm^{-2}$ for 1 h. The mixture (3 ml) was collected and purified using nylon membrane filter (0.2 μm) after adsorption process and lamp exposure. The filterate solution was further analyzed using Shimadzu prominence LC-20 (a high performance liquid chromatography; HPLC equipped with a UV detector and Hypersil GOLD PFP column). The concentration of 2, 4-D and it's intermediate (2, 4-dichlorophenol;

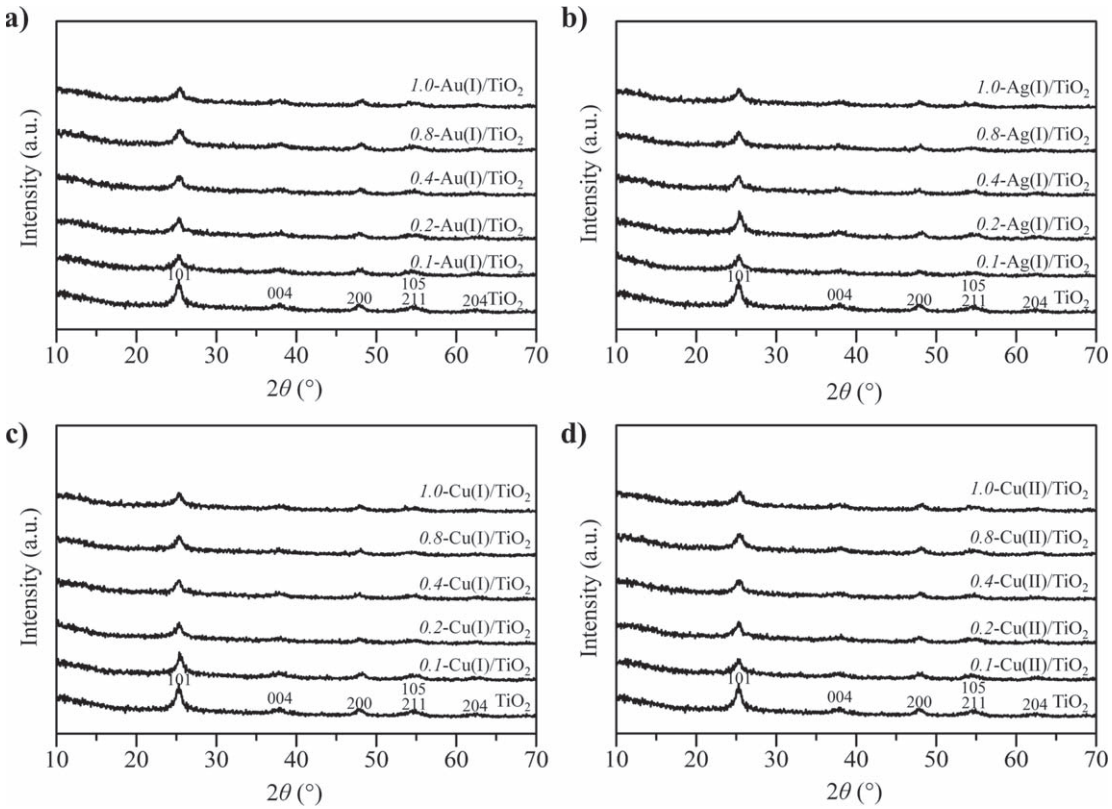

Figure 7. XRD patterns of (a) *x*-Au(I)/TiO_2), (b) *x*-Ag(I)/TiO_2), (c) *x*-Cu(I)/TiO_2), and (d) *x*-Cu(II)/TiO_2 photocatalyst composites.

2, 4-DCP) were examined with an eluent mixture of acetonitrile/distilled water 60:40 (v/v) at 283 nm. The removal percentage and degradation percentage of 2, 4-D was derived from the following equations.

$$\text{Removal of 2, 4-D} = \frac{[2,4\text{-D}]i - [2,4\text{-D}]f}{[2,4\text{-D}]i} \times 100$$

$$\text{Degradation of 2, 4-D} = \frac{[2,4\text{-D}]i - [2,4\text{-D}]f - [2,4\text{-DCP}]}{[2,4\text{-D}]i} \times 100$$

For the above equations, $[2, 4\text{-D}]_i$ is concentration of 2, 4-D before UV irradiation, $[2, 4\text{-D}]_f$ is concentration of 2, 4-D after UV irradiation, and [2, 4-DCP] is concentration of 2, 4-DCP.

3. Results and discussion

3.1. Molecular structure and optical properties of synthesized group 11 metal pyrazolate complexes

The molecular structure of synthesized all M(I or II) pyrazolate complexes were confirmed by using FT-IR spectroscopy. Figure 2 shows that vibration bands of pyrazole ligand for N–H group at 3163 (**1**), 3113 (**1**), 3058(**1**) and 1595 cm^{-1} (**3**) were disappeared compared to that of all pyrazolate complexes. In addition, the new vibration band was observed at 767 cm^{-1} (**6**), which is assigned to the formation of N–Cu–N [18]. These results indicated the complexation reaction of pyrazolate complexes with the base were completely occured.

QTOF LCMSMS is one of the HRMSs that can be used for the exact mass analysis of synthesized organic compounds. Figures 3(a) and (d) shows the observed molecular weight with molecular formula of $C_{15}H_{21}N_6Au_3$ and $C_{10}H_{14}N_4Cu_2$ at 877.0888 and 316.9851 Da for both Au(I) and Cu(II) complexes, which were similar to the isotopic patterns of the calculated molecular formula ($[M + H]^+$) at 877.0903 and 316.9889 Da for Au(I) and Cu(II) complexes. For Ag(I) pyrazolate complex with molecular formula of $C_{15}H_{21}N_6Ag_3$ ($[M + K]^+$) at 644.8613 Da, the particular peak of molecular weight was observed at 643.1092 Da (figure 3(b)). Moreover, the monoisotopic pattern for Cu(I) pyrazolate complex with molecular formula $C_{15}H_{21}N_6Ag_3$ showed a peak at 473.9151 Da (figure 3(c)) for observed molecular weight of $[M]^+$, which was closed to 473.9716 Da of the calculated one. Therefore, M(I or II) pyrazolate complexes were successfully synthesized with high yields.

Figure 4 shows the absorption spectra with a peak tops of 267, 273, 309 and 285 nm for Au(I), Ag(I), Cu(I) and Cu(II) pyrazolate complexes, respectively. These peak tops can be assigned as an absorption edge of the

Table 1. Crystallite size of *x*-Au(I)/TiO_2, *x*-Ag(I)/TiO_2, *x*-Cu(I)/TiO_2, and *x*-Cu(II)/TiO_2 photocatalyst composites.

Composites	Crystallite size[a] (nm)
TiO_2	9.3
0.1-Au(I)/TiO_2	10.0
0.2-Au(I)/TiO_2	10.2
0.4-Au(I)/TiO_2	10.3
0.8-Au(I)/TiO_2	10.2
1.0-Au(I)/TiO_2	10.4
0.1-Ag(I)/TiO_2	9.9
0.2-Ag(I)/TiO_2	10.0
0.4-Ag(I)/TiO_2	10.2
0.8-Ag(I)/TiO_2	10.4
1.0-Ag(I)/TiO_2	10.2
0.1-Cu(I)/TiO_2	9.6
0.2-Cu(I)/TiO_2	9.5
0.4-Cu(I)/TiO_2	9.7
0.8-Cu(I)/TiO_2	9.8
1.0-Cu(I)/TiO_2	10.1
0.1-Cu(II)/TiO_2	9.0
0.2-Cu(II)/TiO_2	9.0
0.4-Cu(II)/TiO_2	9.4
0.8-Cu(II)/TiO_2	9.3
1.0-Cu(II)/TiO_2	9.2

[a] Calculated using Scherrer equation based on 101 lattice plane of anatase TiO_2.

metal complexes containing luminophores with π–π stacking. Moreover, the broad absorption bands at the visible region were usually appeared for the compounds with d-d transition. Such absorption spectra were also supported by the photographs in daylight as shown in the bottom part of figure 4.

By using a peak top from their absorption spectra for the excitation wavelength as shown in figure 4, the luminesent spectra were monitored for all complexes. Figure 5 shows the emission spectra with a peak centered at 471, 686, 590 and 566 nm for Au(I), Ag(I), Cu(I) and Cu(II) pyrazolate complexes, respectively, indicating phosphorescent compounds with the weak metal-metal interactions [15–19]. To support these emission properties, the photographs were captured in the dark room at 254 nm using a UV lamp. As shown at the bottom part of figure 5, the images with dark purple, red, light orange greenish and orange for Au(I), Ag(I), Cu(I) and Cu(II) pyrazolate complexes were in good agreement with the above emission properties.

3.2. Luminescent properties, crystalline structure and morphology of photocatalyst composites

Figure 6 shows absorption spectra of all photocatalyst composites. Absorption band edge of the composites exhibited almost similar with that of anatase TiO_2 (black line). These results demonstrated that pyrazolate complexes might be existed on the surface of the TiO_2. Moreover, absorption peaks of *x*-Au(I)/TiO_2, *x*-Cu(I)/TiO_2, and *x*-Cu(II)/TiO_2 at visible region from 400 to 1000 nm for d-d transition slightly increased with addition of pyrazolate complexes into TiO_2 (inset graph). In contrast, absorption peak at visible region of *x*-Cu(I)/TiO_2 decreased and remain unchanged upon addition of Ag(I) pyrazolate complexes into anatase TiO_2. These results demonstrated that all complexes are stable enough in the preparation of composites.

Figure 7 displays XRD patterns of all photocatalyst composites. It was observed that all diffractograms showed diffraction peaks at 2θ of 25.35°, 38.10°, 48.05°, 54.55° and 62.60° (standard value, JCPDS file No.: 21-1271) which indicates the presence of an anatase phase for TiO_2. As shown in all samples, the intense diffraction peak at 2θ of 25.35° is generally assigned to 101 lattice planes. Estimated crystallite sizes of composites were obtained from Scherrer equation for the main peak as shown in table 1. The crystallite sizes were in the range of 9 to 10 nm where it was almost similar to that of the bulk TiO_2. Hence, these results suggested that addition of M(I or II) pyrazolate complexes have not affected the structural properties of anatase TiO_2 in their composites [12–15]

Figure 8 shows FESEM images of selected 0.4-M(I or II)/TiO_2 composites. The visualization showed that 0.4-Au(I)/TiO_2 composite displayed some particles with same shape and size (figure 8(a)), which is almost similar to the morphology of anatase TiO_2 [12]. Moreover, all other 0.4-M(I or II)/TiO_2 composites with Ag(I), Cu(I) and Cu(II) showed some aggregation of particles with different shapes and sizes (figures 8(c), (e), (g)). Further investigation on the dispersion of M(I or II) pyrazolate complexes in the composites was carried out with

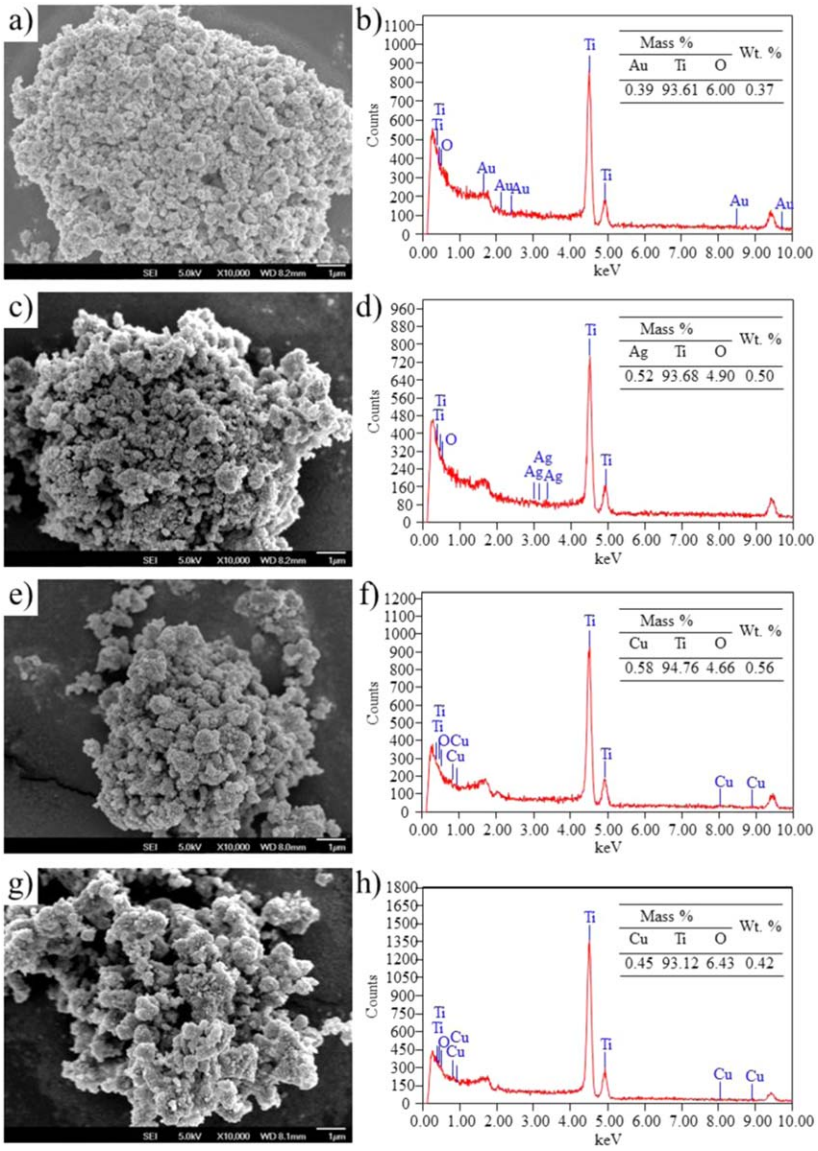

Figure 8. (a), (c), (e), (g) FESEM images and (b), (d), (f), (h) EDX spectra of (a), (b) 0.4-Au(I)/TiO_2, (c), (d) 0.4-Ag(I)/TiO_2, (e), (f) 0.4-Cu(I)/TiO_2, and (g), (h) 0.4-Cu(II)/TiO_2.

EDX analysis (figures 8(b), (d), (f), (g)) where the insert tables were summarized the mass percentage of respective elements. The insert tables showed that weight percentage of 0.4-M(I or II)/TiO_2 composites were almost closed to the loading of the complex to TiO_2. Hence, such impregnation method is good enough on the preparation of luminescent photocatalyst nanocomposite.

TEM measurements were performed to study the morphology of the composites. In figure 9, the morphology of selected 0.4-M(I or II)/TiO_2 composites (figures 9(b)–(e)) showed almost similar to that of anatase TiO_2 (figure 9(a)). Moreover, the particle size in all images of the composites was in good agreement with the crystallite sizes value as shown in table 1. These results indicate that small amount of complexes was dispersed well in anatase TiO_2 composites.

Figure 10 shows the emission properties of all photocatalyst composites. As discussed above, upon excited at the peak top of its excitation spectrum, it gave an emission peak centered (black dashed line) at 686, 471, 590 and 566 nm for Au(I), Ag(I), Cu(I) and Cu(II) pyrazolate complexes, respectively, due to the intermolecular metal-metal interaction [15–22]. On the other hand, photocatalyst composites showed a broad emission band with two peaks at 420 and 466 nm, which are corresponding to the emission of TiO_2. When loading amount of M(I or II) pyrazolate complexes were increased, the emission intensity of the composites at 420 and 466 nm were reduced for all composites. Such phenomena might be due to the suppression of electron-hole recombination process as report previously [12–15] where the electron from valance band of TiO_2 will be transferred to the columnar assembly of metal complexes. Although all pyrazolate complexes were incorporated onto the surface of TiO_2, the

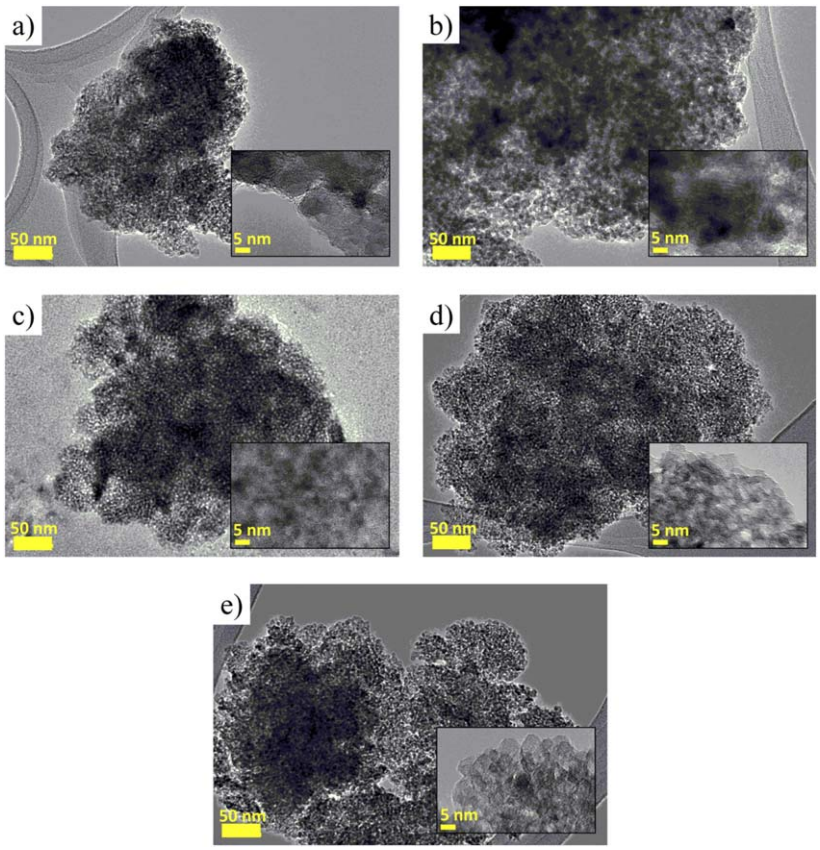

Figure 9. TEM images of (a) anatase TiO_2, (b) 0.4-Au(I)/TiO_2), (c) 0.4-Ag(I)/TiO_2), (d) 0.4-Cu(I)/TiO_2), and (e) 0.4-Cu(II)/TiO_2.

emission peak of M(I or II) pyrazolate complexes was not observed on all composites. These results suggested that low loading amount of pyrazolate complexes might not influenced TiO_2 structure.

3.3. Photocatalytic activity of photocatalyst composites

The performance of luminescent group 11 metal pyrazolate complexes/titanium oxide composites (*x*-M(I or II)/TiO_2) as a photocatalyst were evaluated using 2, 4-D as a model pollutant under a UV irradiation at ambient temperature in 1 h. Prior to this photocatalytic reaction, the equilibrium of adsorption-desorption process was firstly performed so that the adsorption efficiency was not involved in the calculation of photocatalytic activity. Based on stability test under UV light irradiation with M(I or II) pyrazolate complexes only and without photocatalyst, the degradation of 2, 4-D was not occurred due to lack of hydroxyl radical ($\bullet OH^-$) in the reaction system. By using standard calibration curve equation of 2, 4-D and 2, 4-DCP with the previous equations above ($y = 2,716,584x + 1263$, $y = 2{,}915{,}622x + 5829$; respectively), the concentration of 2, 4-D and 2, 4-DCP in the testing can be determined.

Figures 11(a) and (b) shows the photocatalytic testing of the photocatalyst composites where the removal and degradation percentages were evaluated. It showed that addition of M(I or II) pyrazolate complexes was found to give significant improvement in the photocatalytic activity of anatase TiO_2 even in 1 h. In particular, the composites 0.4-Au(I)/TiO_2 and 0.4-Ag(I)/TiO_2 gave the highest removal in 85% and degradation in 36% compared to anatase TiO_2 (49% and 10%, respectively). Interestingly, the composite Cu(I)/TiO_2 with 0.4 wt% gave even better removal in 99% and almost the same percentage of the degradation. In contrast, composites with complexation of Cu(II) ions by using the same ligand was found to show an enhancement in the degradation of 2, 4-D from 36% to 48%. The efficiency in removal of 2, 4-D (99%) for the composite Cu(II)/TiO_2 with 0.4 wt% as a photocatalyst was involved by its degradation efficiency (48%) where the produced 2, 4-DCP was found to be around 51%. These results showed that trinuclear Au(I), Ag(I) and Cu(I) pyrazolate complexes in anatase TiO_2 composites will significantly improve the photocatalytic activity of TiO_2 due to the reduction of electron-hole recombination of TiO_2 (as shown in figure 10). Moreover, trinuclear Cu(I) pyrazolate complexes with longer metal-metal distance in composites as shown from the peak top of its emission spectrum (590 nm) for electron transfer from conduction band of TiO_2 is responsible for such performance in

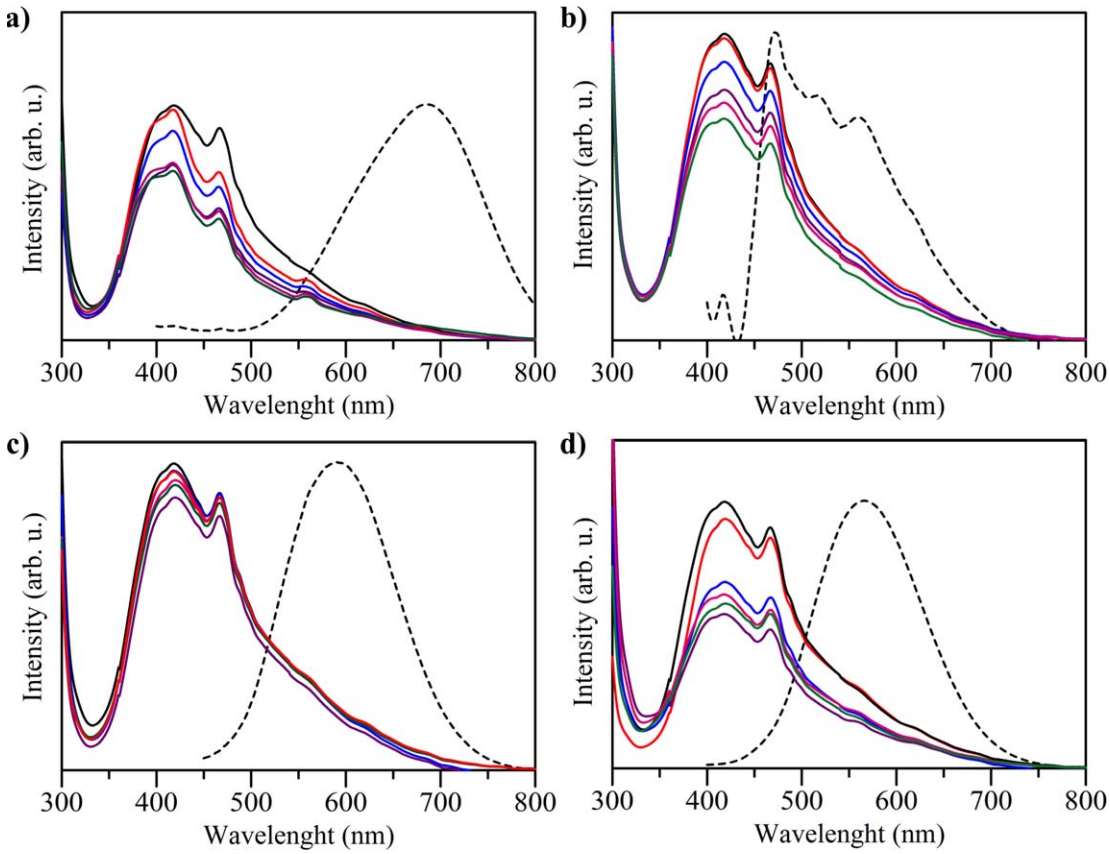

Figure 10. Emission spectra of (a) Au(I), (b) Ag(I), (c) Cu(I) and (d) Cu(II) pyrazolate complexes (black dashed line), TiO_2 (black line) and photocatalyst composites (0.1, 0.2, 0.4, 0.8, 1.0-M(I or II)/TiO_2; red, blue, purple, orange and green lines).

the removal. Indeed, dinuclear Cu(II) pyrazolate complex with less rigid structure has more longer metal-metal distance (emission wavelength at 566 nm) to give such better performance in the degradation. In addition, further addition up to 1.0 wt% of M(I or II) pyrazolate complexes slightly decreased the activity of TiO_2. Based on emission spectra in figure 10 and photocatalytic activity in figure 11, it can be proposed that the presence of small amount of M(I or II) pyrazolate complexes with a metal-metal distance in the columnar structure for light emission properties might play an important role to reduce the electron-hole recombination on TiO_2. The columnar assembly of the metal complexes with a *chair-like* coordination geometry as reported previously [15–22] is designed to trap the electron from the valance band of TiO_2 while the molecular structure promotes the performance of the photocatalyst for the degradation of the pollutant.

Figure 11(c) shows kinetic study of the composites for the removal of 2, 4-D at 15, 30, 45 and 60 mins. It was found that the removal of 2, 4-D could be fitted with the first order kinetic equation,

$$\frac{dC}{dt} = -kC \tag{1}$$

$$\ln C = -kt + \ln C_0 \tag{2}$$

which C and C_0 is final and initial concentrations of 2, 4-D, respectively and k is rate constant. This kinetic study showed that addition of M(I or II) pyrazolate complexes increased the k of TiO_2 (0.0105 min^{-1}) about 3 times for 0.4-Au(I)/TiO_2 (0.0327 min^{-1}) and 0.4-Ag(I)/TiO_2 (0.0317 min^{-1}) composites and 6 times for 0.4-Cu(I)/TiO_2 (0.0619 min^{-1}) and 0.4-Cu(II)/TiO_2 (0.0655 min^{-1}). Moreover, the photocatalyst composite 0.4-Cu(II)/TiO_2 gave the highest k value compared to other composites where it was in good agreement with its highest photocatalytic activity (figure 11(a)). Indeed, such first order kinetic in the photocatalytic removal of 2, 4-D was also found with other photocatalysts in the previous reports [23–25].

Photocurrent measurement was carried out to study the higher activity of the 0.4-Cu(II)/TiO_2 composite compared to anatase TiO_2. A shown in figure 12, the photocurrent density of SPE substrate coated with 0.4-Cu(II)/TiO_2 composite showed a significant improvement around 2 times in the photocurrent density compared to anatase TiO_2. This photocurrent measurement for the composite was only dropped at first cycle and then was stable enough for each light-on/off event. Such higher density in the composite indicates that electron-hole pairs were generated in longer lifetime compared to in the anatase TiO_2 [12, 26]. These results also

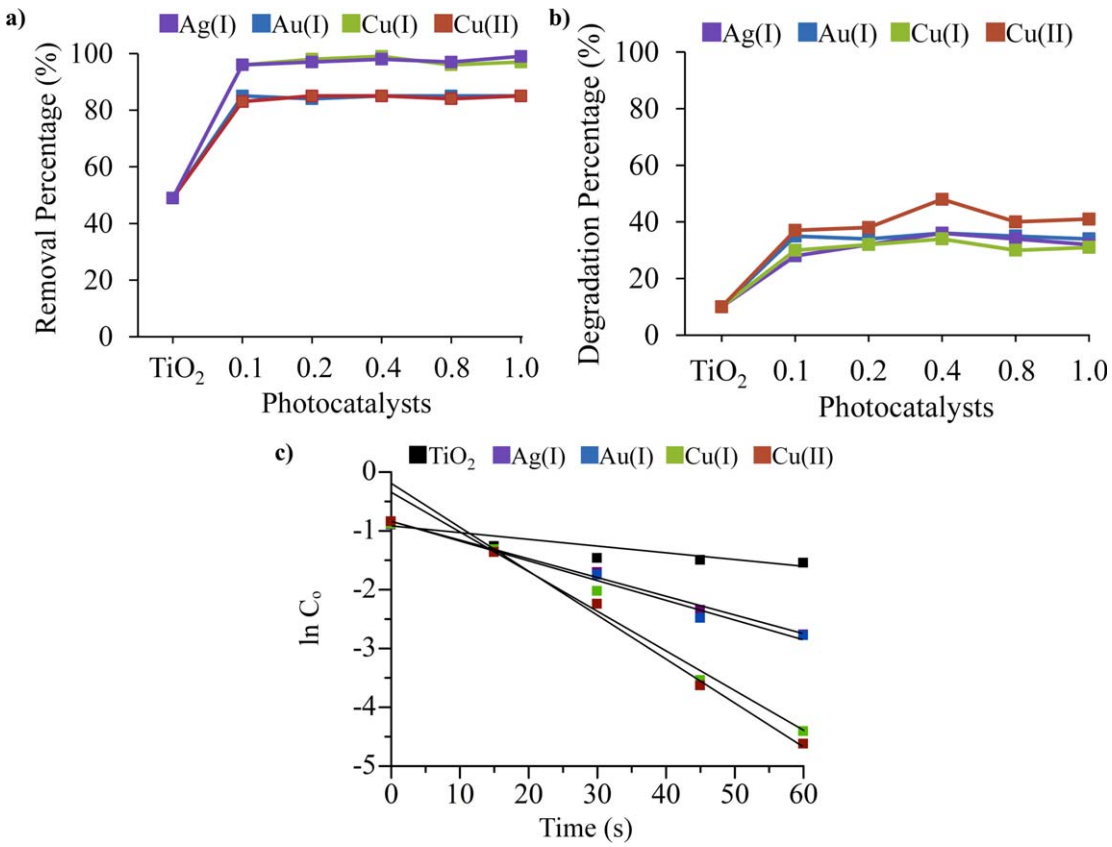

Figure 11. Photocatalytic activity based on the (a) removal and (b) degradation percentage versus photocatalysts for all composites and anatase TiO_2 as well as (c) their kinetic study based on the removal for composite with 0.4 wt% of M(I or II) pyrazolate complexes.

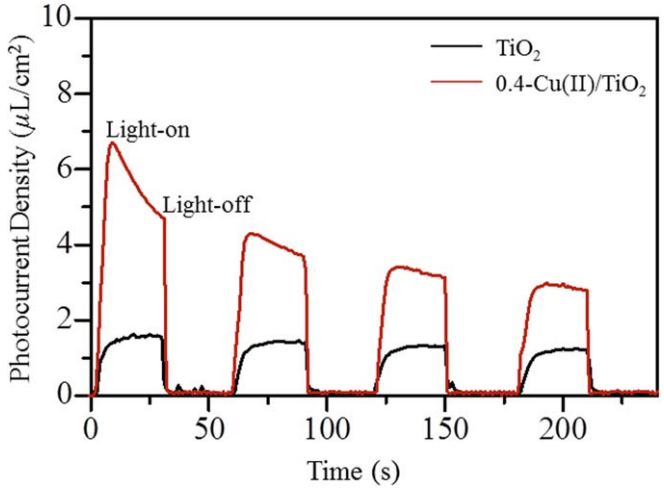

Figure 12. Photocurrent density versus time respond of anatase TiO_2 and 0.4-Cu(II)/TiO_2 composite.

indicate that the presence of Cu(II) pyrazolate complex in the composite effectively decreased electron-hole recombination process, thus gave much higher photocatalytic activity compared to anatase TiO_2.

In development of good photocatalysts, the stability is an important factor in the photocatalytic reactions as shown from unchanged photocatalytic activity while the chemical structure and morphology properties should remain the same. A series of experiment were done to study the stability of the photocatalyst composites with the evaluation of removal and degradation percentages for three cycles. As shown in figure 13, the photocatalytic activity of all composites almost provided the same results with only reduce in less than 5%. These results indicate the complexes in the TiO_2 composites are stable enough to work as photocatalysts.

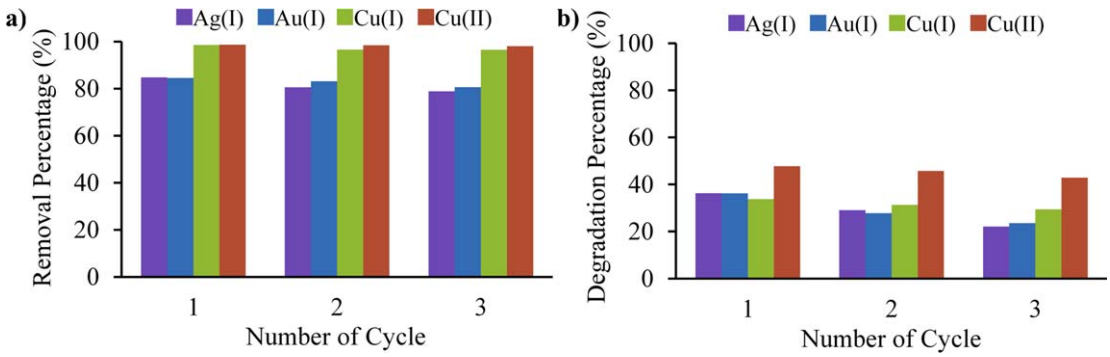

Figure 13. Photocatalytic stability experiments based on the (a) removal and (b) degradation percentage versus number of cycle for all composites with 0.4 wt% of M(I or II) pyrazolate complexes.

4. Conclusion

In conclusion, M(I or II) pyrazolate complexes in high yields were successfully synthesized by the complexation of 3, 5-dimethyl pyrazole ligand with different metal salt of group 11 where all complexes showed phosphorescent properties originating from the weak metal-metal interactions. A series of M(I or II) pyrazolate complexes/titanium oxide composites (x-M(I or II)/TiO_2) with various loading amount of M(I or II) pyrazolate complexes (x = 0.1, 0.2, 0.4, 0.8, and 1.0 wt%) were prepared by using a simple impregnation method. Addition of M(I or II) pyrazolate complexes was not much affected the morphology and crystallite size of anatase TiO_2. In addition, presence of M(I or II) pyrazolate complexes also reduced the emission intensity of TiO_2. 0.4 x-M(I or II)/TiO_2 composite showed the highest removal and degradation of 2, 4-D compared to TiO_2. This result demonstrated that optimum amount of M(I or II) pyrazolate complexes might act as an efficient modifier for anatase TiO_2, thus improved the photocatalytic activity. Interestingly, x-Cu(II)/TiO_2 showed the better degradation of 2, 4-D with 48% compared to other x-M(I)/TiO_2 and TiO_2 composites (36% and 10%; respectively). This work demonstrated that modification of TiO_2 with phosphorescent group 11 pyrazolate complexes at the molecular level (different metal ions and rigidity) as photocatalyst composites is a new approach to enhance photocatalytic activity of organic pollutants.

Acknowledgments

The work was partially financed by Directorate General of Science and Technology Resources and Higher Education, Ministry of Research, Technology, and Higher Education, The Republic of Indonesia for fine-tuning publications under World Class Professor (WCP) Program 2018, Scheme B with a contract number 123.51/D2.3/KP/2018. The same ministry through Competency Based Research (PBK) Grant 2018 with a contract number 013/MACHUNG/LPPM/SP2H-LIT/II/2018 through Directorate General of Strengthening Research and Development was also acknowledged for the financial support. Moreover, N H Sabran also acknowledges Ministry of Higher Education (MOHE), Malaysia through MyBrain15 Scholarship (MyPhD) for the financial support in the doctoral study. We also thank Dr Faisal Hussin for the photocurrent measurement.

ORCID iDs

Hendrik O Lintang https://orcid.org/0000-0002-1911-8100
Siew Ling Lee https://orcid.org/0000-0002-7325-0321
Leny Yuliati https://orcid.org/0000-0003-1600-5757

References

[1] Hoffmann M R, Martin S T, Cho W and Bahnemann D W 1995 *Chem. Rev.* **95** 69
[2] Choi W 2006 *Catal. Surv. Asia* **10** 16
[3] Fujishima A, Zhang X and Tryk D A 2008 *Surf. Sci. Rep.* **63** 515
[4] Ohno K, Sarukawa K, Tokieda K and Matsumura M 2001 *J. Cat.* **203** 82
[5] Rui Z, Wu S, Peng C and Ji H 2014 *Chem. Eng. J* **243** 254
[6] Siah W R, Lintang H O, Shamsuddin M and Yuliati L 2016 *IOP Conf. Ser. Mat. Sci. Eng.* **107** 012005
[7] Di Paola A, Marcì G, Palmisano L, Schiavello M, Uosaki K, Ikeda S and Ohtani B 2001 *J. Phys. Chem. B* **106** 637

[8] Dvoranová D, Brezová V, Mazúr M and Malati M A 2002 *Appl. Catal. B: Environ* **37** 91
[9] Teh C M and Mohamed A R 2011 *J. Alloys and Comp* **509** 1648
[10] Tang Y, Luo S, Teng Y, Liu C, Xu X, Zhang X and Chen L 2012 *J. Hazard. Mater.* **241–242** 323
[11] Peter A, Mihaly-Cozmuta L, Mihaly-Cozmuta A, Nicula C, Tudoran L B and Baia L 2014 *Mater. Tech.: Adv. Performance Mater* **29** 129
[12] Siah W R, Lintang H O, Shamsuddin M, Yoshida H and Yuliati L 2016 *Catal. Sci. Technol* **6** 5079
[13] Yuliati L, Siah W R, Roslan N A, Shamsuddin M and Lintang H O 2016 *Malaysian J. Anal. Sci.* **20** 171
[14] Roslan N A, Lintang H O and Yuliati L 2015 *Adv. Mater. Res* **1112** 180
[15] Lintang H O, Roslan N A, Ramlam N, Shamsuddin M and Yuliati L 2016 *Mater. Sci. Forum* **846** 697
[16] Enamoto M, Kishimura A and Aida T 2001 *J. Am. Chem. Soc.* **123** 5608
[17] Rasika Dias A V, Diyabalanage H V K, Eldabaja M G, Elbjeirami O, Rawashdeh–Omary M A, Franzman M A and Omary M A 2005 *J. Am. Chem. Soc.* **127** 7489
[18] Ghazalli N F, Yuliati L, Endud S, Shamsuddin M and Lintang H O 2014 *Adv. Mater. Res* **970** 44
[19] Lintang H O, Ghazalli N F and Yuliati L 2017 *Indones. J. Chem* **17** 191
[20] Cingolani A, Galli S, Masciocchi N, Pandolfo L, Pettinari C and Angelo Sironi T 2005 *J. Am. Chem. Soc.* **127** 6144
[21] Lintang H O, Kinbara K, Yamashita T and Aida T 2012 *Int. Conf. on ESciNano 2012—Proc. 2012, IEEE proceedings (Johor, Malaysia, 2012)* 6149684 (https://doi.org/10.1109/ESciNano.2012.6149684)
[22] Lintang H O, Yuliati L and Endud S 2014 *Mater. Res. Innov.* **18** S6–444
[23] Carcel A R, Andronic L and Duta A 2012 *Mater. Charact.* **70** 68
[24] Tang Y, Luo S, Teng Y, Liu C, Xu X, Zhang X and Chen L 2012 *J. Hazard. Mater.* **241–242** 323
[25] Akpan U G and Hameed B H 2011 *Chem. Engineer. J* **173** 369
[26] Byeon J H and Kim J-W 2014 *J Matter. Chem* **2** 6939